Proceedings of the 10th International Conference on Civil Structural and Transportation Engineering (ICCSTE 2025)
July, 2025 | Imperial College London Conference Center, London, United Kingdom
Paper No. 368
DOI: 10.11159/iccste25.368

Numerical Investigation of Fluid–Structure Interaction in LNG Storage Tanks under Seismic Loading

Shafqat Ullah[1], Iraj H. P. Mamaghani[2]
[1]University of North Dakota
Department of Civil Engineering
243 Centennial Drive, Stop 8115, Grand Forks 58203, USA
shafqat.ullah@und.edu; iraj.mamaghani@und.edu

Abstract **-** The seismic safety of liquid-filled cylindrical storage tanks is vital for the energy infrastructure, particularly in high seismic zones. This study presents a high-fidelity finite element analysis (FEA) of LNG storage tank system, comprising an inner steel tank and outer reinforced concrete tank. Given the complex nature of fluid-structure interaction (FSI) and the risk of sloshing-induced instability during seismic events, the objective is to provide a comprehensive numerical framework to assess the structural response under realistic earthquake loading conditions. The Arbitrary Lagrangian-Eulerian (ALE) approach is employed to capture the dynamic interaction between the tank structure and the contained fluid, allowing for accurate simulation of sloshing behavior and hydrodynamic pressures. For simplicity, water is used as the infilled liquid. The Concrete Damage Plasticity (CDP) model is adopted for the concrete components to account for nonlinear material degradation under seismic loading. Although the LNG storage system modeled in this study consists of outer reinforced concrete containment, the analysis primarily focuses on the inner tank's seismic response and associated fluid-structure interaction (FSI). The simulation results reveal that while the inner steel tank maintains stable performance under static conditions, dynamic loading produces transient stresses, localized deformation, and significant sloshing wave heights. given that the dynamic loading did not result in significant damage in compression and cracks in tension in the outer tank, detailed discussion on its behavior was omitted to maintain clarity and focus on the more critical inner steel containment. These findings emphasize the critical role of FSI in amplifying structural demands and demonstrate the need to go beyond conventional static or simplified dynamic methods typically used in design codes. This study offers valuable insights into the seismic behavior of LNG tanks and contributes to the advancement of performance-based seismic design practices for critical storage infrastructure.

Keywords**:** LNG Tanks, Local Buckling, Non-Linear Buckling Analysis, Fluid-Structure Interaction, Liquid Sloshing, Hydrodynamic Pressure, Seismic Excitation, ABAQUS.

1. Introduction

With the growing global demand for natural gas in recent years, liquefied natural gas (LNG) storage tanks have emerged as critical components of urban energy infrastructure. These tanks are commonly constructed in coastal regions as illustrated in Fig. 1 [3], many of which are characterized by high seismic activity, thereby raising concerns about their structural safety

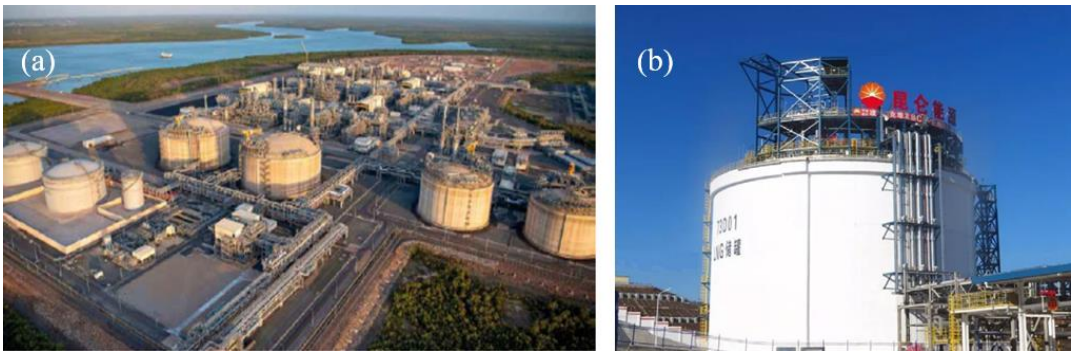

Fig. 1(a): LNG terminal facility [2], and (b). Typical full-containment LNG storage tank [2]

and operational resilience during earthquake events [1,2]. Due to their thin-walled geometry, cylindrical steel LNG storage tanks are particularly susceptible to local buckling under seismic loading. Moreover, they pose significantly higher seismic

risks compared to conventional buildings, as their failure can lead to secondary hazards such as explosions, fires, and environmental contamination, potentially resulting in extensive property damage and loss of human life.

Several researchers have investigated the static and dynamic buckling behavior of cylindrical steel storage tanks, with particular emphasis on their structural stability under various loading conditions, including seismic and wind-induced excitations [3-9]. Chen et al., [10] investigated the seismic performance of large-scale LNG storage tanks through experimental methods. Their findings indicated that the acceleration response of the tanks exhibited an approximately linear increasing trend along the height of the tank. Ullah and Mamaghani, [11] and Zhang et al., [12] conducted a three-dimensional finite element analysis (FEA) to evaluate the seismic performance of LNG storage tanks. The study examined key response parameters, including displacement–time histories, acceleration time histories, and the distribution of hydrodynamic pressure along the tank height. The results revealed that the hydrodynamic pressure reached its maximum near the base of the tank, which may lead to local yielding and elevated equivalent plastic strain concentrations in the bottom region. Ullah and Mamaghani, [13] conducted a detailed three-dimensional finite element analysis to investigate the seismic performance of three different cylindrical steel storage tanks, with particular emphasis on FSI. The study employed a coupled acoustic–structure interaction (CAS) approach within the finite element framework to accurately capture the dynamic behavior of the liquid-filled tanks under seismic loading. Liu et al., [14] experimentally evaluated the seismic performance of LNG storage tanks, explicitly accounting for FSI. Their findings revealed that liquid sloshing significantly influences the hydrodynamic pressure response, with the magnitude of this effect decreasing as the liquid depth increases. Similarly, Ullah and Mamaghani, [15,16] conducted a numerical investigation on the seismic performance of LNG tanks, focusing on the effects of liquid sloshing under varying seismic input motions. Their study emphasized the importance of accurately capturing sloshing dynamics to predict pressure distribution and structural demand in liquid-filled storage tanks during earthquake loading. Sharari et al., [17] conducted a (FEA) to investigate the seismic performance of full-containment LNG storage tanks subjected to various ground motion records.

Despite tremendous progress in assessing LNG storage tanks' seismic performance, a number of obstacles still stand in the way of accurately describing the intricate physical behavior of these systems under strong ground motions. Although previous research has yielded important insights, many of these models have used oversimplified assumptions that ignore important interactions such dynamic sloshing and FSI. The interaction between the flexible tank wall and internal fluid motion can be accurately modeled using the ALE technique, particularly when input peak ground accelerations (PGAs) varies. However, more investigation is necessary to use reliable ALE-based simulations to comprehensively evaluate the impact of sloshing-induced impact pressures, liquid height fluctuations, and nonlinear structural response. This study proposes a high-fidelity FE model utilizing ABAQUS to assess the seismic performance of LNG tanks subjected to different ground motion intensities in order to increase the seismic resilience and design dependability of LNG storage facilities. In order to simulate significant deformations of the liquid free surface and structural elements, as well as the dynamic forces induced by fluid sloshing during seismic excitation, the ALE approach is used to precisely capture the interaction between the inner tank wall and liquid contained.

2. Finite Element Modeling

A high-fidelity finite element model of the LNG storage system was developed in ABAQUS/Explicit to evaluate its seismic response under varying ground motion intensities. The ALE formulation was employed to accurately simulate the FSI between the internal liquid domain and the tank walls. The ALE approach within the finite element method provides a robust and efficient framework for such applications. In the context of seismic analysis of liquid storage tanks, the ALE formulation effectively accommodates large deformations of both the free surface of the fluid and the structural boundaries. It also facilitates accurate prediction of hydrodynamic forces resulting from the coupled response of the flexible tank and the contained liquid, including sloshing-induced pressure impacts on the tank walls and roof [18]. Further details and various applications of the ALE formulation are comprehensively discussed in the literature [19–21].

The inner steel tank (Primary containment), characterized by its thin-walled geometry and flexibility, was modeled using S4R shell elements—a 4-node, doubly-curved, reduced-integration shell element suitable for nonlinear large-deformation problems. The outer reinforced concrete tank (secondary containment) was modeled using C3D8R solid

elements as illustrated in Fig 2(b), which are 8-node linear brick elements with reduced integration. Steel reinforcement is modeled using T3D2 elements, which are two-node three-dimensional truss elements. These rebars are embedded within the concrete tank to simulate the bond interaction and ensure composite structural behavior

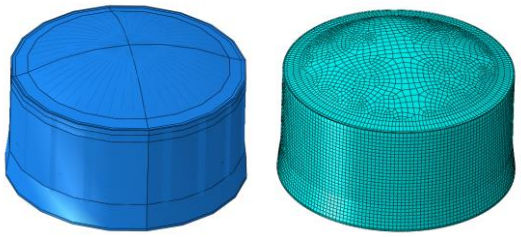

(a) (b)

Fig. 2 (a): Assembly of the inner and outer Tank, and (b): FE Meshing

2.1. Material and Geometric Configurations

The cylindrical inner tank is constructed from steel, and the outer tank is composed of reinforced concrete; their geometric properties are summarized in Table 1. The material properties [22] of both steel inner Tank and the reinforcement in the outer concrete Tank are shown in Table 2. The density (ρ) and bulk modulus (K_L) of the infilled liquid is taken as (ρ = 1000 kg/m3), and 2210 MPa, respectively. The cylindrical inner steel tank and the concrete outer tank are assembled as shown in Figure 2 (a). Fig. 3 illustrates both the original and modified stress–strain curves of the rebars [12], from which the modified curve was adopted in this study.

Table 1: Geometric and material properties of inner steel and outer concrete Tanks

Specimen	Geometric Configuration					Material properties	
	H (m)	*R (m)*	Liquid filled (H_L)	Thickness *(m)*		Density (ρ) kg/m^3	Poisson's ratio (v)
				Lower thickness (t_1)	Upper thickness (t_1)		
Steel	2.54	2.980	1.20	0.005	0.005	7850	0.30
Concrete	2.78	2.985	–	0.119	0.065	2400	0.20

Table 2 : Material properties [22] of the steel inner Tank and reinforcement in outer concrete Tank

Specimen	Elastic modulus (Mpa)	Yield strength (Mpa)	Ultimate strength (Mpa)	Ultimate strain
Steel inner Tank	172,000	395	592	0.14
Steel rebars	205,000	352	596	0.15

2.2. Concrete Damage Plasticity (CDP) model

The CDP model is extensively recognized an accurate and practical constitutive framework for simulating the nonlinear behavior of concrete, particularly effective in capturing failure modes governed by tensile cracking and compressive crushing [23]. The density and the poison's ratio of concrete are given in Table 1. The plasticity parameters used in CDP model in ABAQUS are illustrated in Table 3 [23]. Inelastic behavior of concrete is defined using damage parameters and associated inelastic strains for compression and cracking strain in tension. The input parameters used in the CDP model include a dilation angle of 30°, eccentricity of 0.1, and a viscosity parameter of 0.0001, among others as given in Table 3.

These values are commonly adopted to balance convergence and accuracy when simulating concrete under dynamic and cyclic loading conditions. The plasticity parameters and damage evolution data enable a more realistic simulation of concrete behavior and stiffness degradation, which is critical in seismic analysis.

Table 3. Plasticity parameters used in CDP model [23]

Plasticity parameters	
Dilation angle	30
Eccentricity	0.1
Fb0/fc0	1.16
K	0.667
Viscosity parameter	0.0001

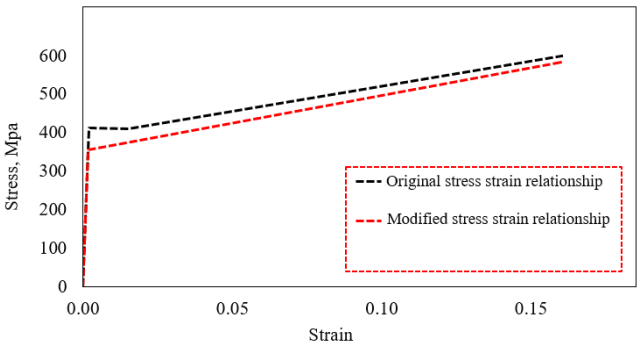

Fig. 3: Stress vs strain curve [12]

2.3. Loading, and Boundary Conditions (BCs)

The numerical analysis was performed in two sequential steps. In the first step, a nonlinear static Riks analysis was conducted to evaluate the response of the liquid-filled tank under static loading. This was followed by a second step involving a dynamic explicit analysis to assess the tank's seismic response. The initial hydrostatic loading step was applied over a duration of 2 seconds to capture the nonlinear behavior under static pressure. In the next step, a dynamic explicit analysis was carried out and the ground motion time-history data from the real earthquake events—the Takatori earthquake, 1976 Friuli (Italy), 1994 Northridge , and Emeryville earthquakes were applied as horizontal base excitations. These seismic inputs were incorporated through boundary conditions using acceleration–time records expressed in terms of g (where g = 9.81 m/s²) in the horizontal direction. Appropriate BCs were applied to simulate realistic tank behavior under seismic loading. All degrees of freedom at the tank base were restrained, except for the horizontal translational direction in which the ground motion excitations were applied. This configuration allows free movement in the direction of the seismic input while preventing vertical and out-of-plane displacements or rotations, thereby representing an anchored base condition.

3. Results and Discussion

The finite element (FE) program ABAQUS is used to assess the performance of cylindrical storage tanks under both static and dynamic loading. The analysis focuses on evaluating the deformation response, stress distribution, and the liquid sloshing vs time response of inner steel tank when subjected to four different real-world earthquakes loading. The results demonstrate that the tank does not experience significant deformation under static loading, with the maximum von Mises stress reaching approximately 2.11 MPa. The stress distribution under these conditions is relatively uniform and primarily concentrated just above the tank base, as illustrated in Fig. 4. Although the static analysis confirms minimal deformation and a uniform stress distribution, the dynamic analysis reveals a significantly more complex structural response. It captures the effects of FSI, transient stresses (time-dependent stresses) induced by

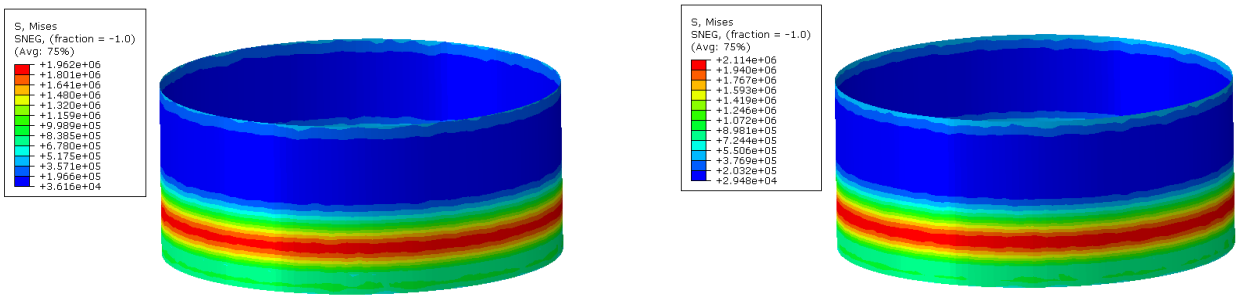

Fig. 4: Stress variation with respect to time in inner steel tank subjected to static loading

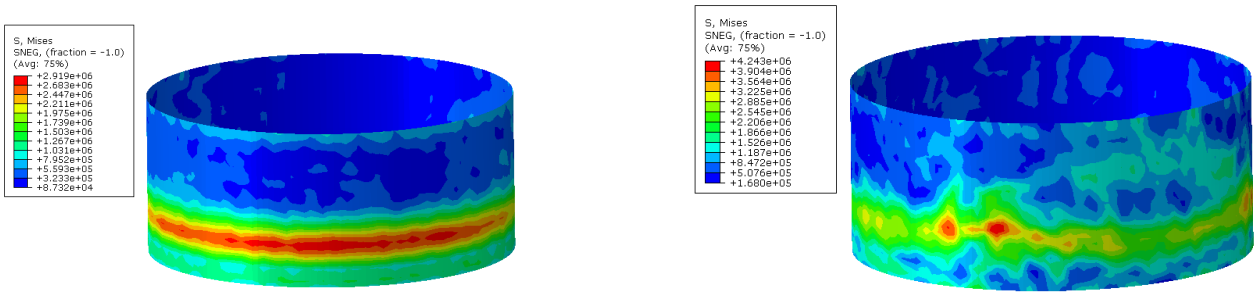

Fig 5: Stress variation with respect to time under Takatori Earthquake

earthquake-induced hydrodynamic pressure distribution along the tank height—as well as sloshing of the contained liquid. These dynamic stresses are considerably more critical and can lead to local yielding or instability, particularly in thin-walled

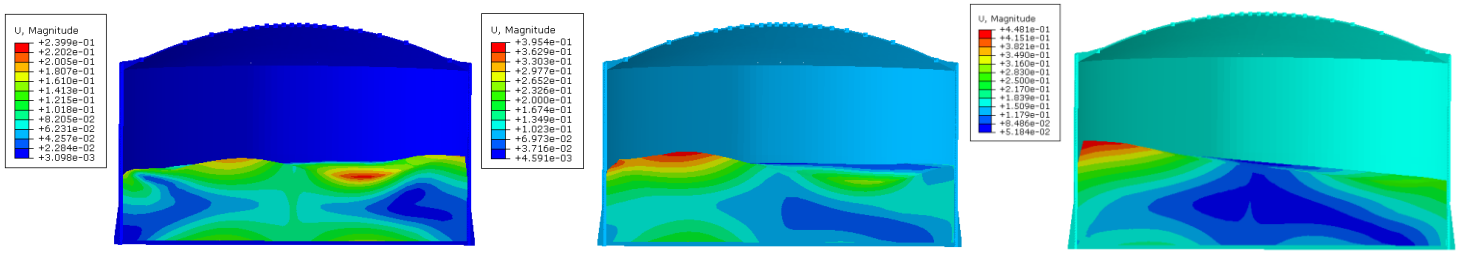

Fig. 6: Deformation contour of Tank subjected to Takatori Earthquake

steel tanks, highlighting the importance of accounting for such effects in seismic design. Fig. 5 illustrates the von mises stress contour plots and its variation with respect to time when the tank subjected to Takatori earthquake. Fig. 6 presents the displacement contour plots of the cylindrical steel tank subjected to the Takatori earthquake, captured at different time intervals to reflect the deformation behavior of the storage tank. The liquid inside the tank exhibits dynamic behavior,

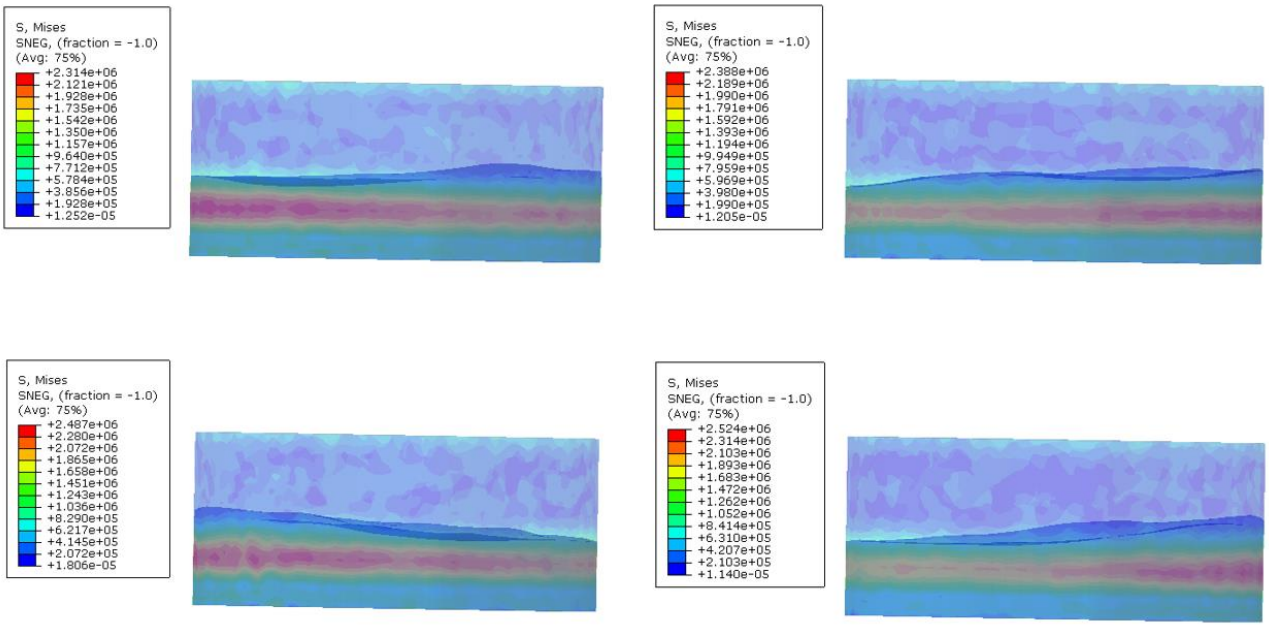

Fig 7: Stress variation with respect to time under NR Earthquake

commonly referred to as liquid sloshing, which induces dynamic pressure (convective pressure component) near the free surface. Similarly, the deformation response and stress distribution of tank subjected to Northridge as shown in Fig. 7, and Emeryville earthquake are also evaluated. The results reveal that the tank experiences a peak von Mises stress of 4.24 Mpa under the Takatori earthquake, which exhibited the most intense dynamic excitation among the considered ground motions. Compared to the results from Takatori earthquake, the stress magnitudes were noticeably lower under the other seismic inputs, with maximum stresses of 2.46 MPa, 2.75 MPa, and 2.52 MPa recorded for the Emeryville, Friuli, and Northridge earthquakes, respectively. This reduction in stress levels reflects the relative severity and frequency content of each ground

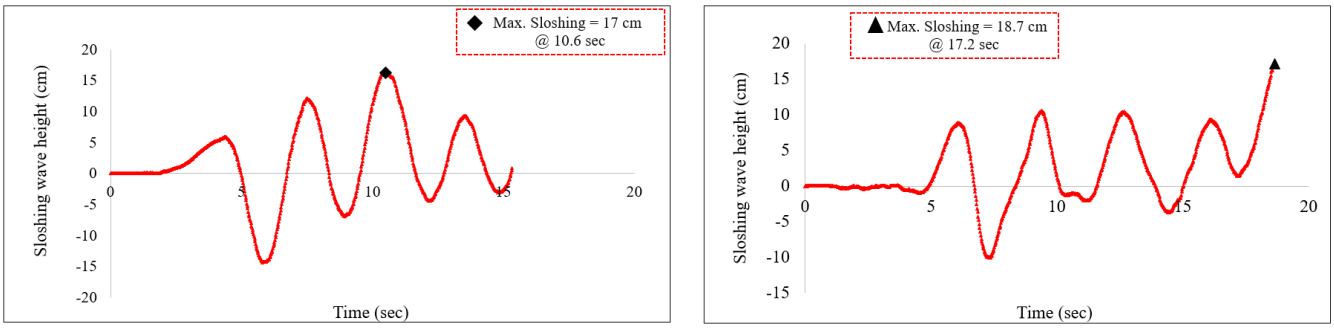

(a) (b)

Fig 8. Sloshing vs Time response, (a): Friuli Earthquake, (b): Emeryville Earthquake

motion, highlighting the critical role of earthquake characteristics in influencing the structural response of liquid-filled storage tanks. Furthermore, the time-history response of the liquid sloshing wave height was examined for all considered seismic excitations to assess its effects on dynamic behavior of the LNG tank. As shown in Fig. 8(a), the Friuli earthquake produced a peak sloshing height of approximately 17.0 cm at 10.6 seconds, while the Emeryville earthquake, illustrated in Fig. 8(b), resulted in a maximum wave height of 18.7 cm occurring at 17.2 seconds. These sloshing responses exhibit noticeable oscillatory motion due to the convective components of the liquid's dynamic interaction with the tank walls. The Northridge earthquake further intensified this behavior, generating the highest sloshing wave height among the considered inputs, reaching 24.10 cm, as shown in Fig. 9. This variation in sloshing magnitude underscores the influence of ground motion characteristics particularly frequency content and duration—on fluid motion within the tank.

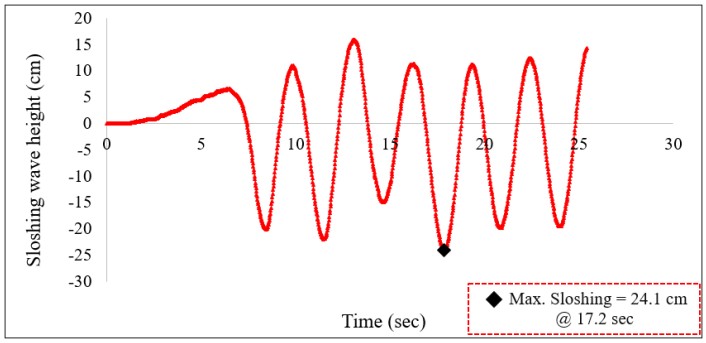

Fig 9: Sloshing vs Time response of tanks subjected to Northridge Earthquake

4. Conclusion

This study presented a detailed finite element analysis (FEA) using the commercial software ABAQUS to assess the seismic performance of LNG storage tanks, with a particular emphasis on FSI. To accurately capture the coupled behavior between the liquid and the thin-walled inner steel tank, the ALE formulation was employed. This approach enabled the simulation to account for large deformations and the dynamic free-surface motion of the liquid, thereby providing a more realistic representation of seismic loading effects. The analysis primarily focuses on the inner tank's seismic response, associated FSI, hydrodynamic induced stresses, deformation response as well as the evaluation of nonlinear sloshing behavior of tank under different input seismic intensities. The key findings observed from this research are summarized below.

- The nonlinear static analysis revealed that the tank remains structurally stable under hydrostatic loading, with stress concentrations localized near the base and lower wall regions.
- The response of the tank varied significantly when subjected to seismic excitations. It was noticed that the highest von Mises stress reached 4.24 MPa, when storage tank subjected to Takatori earthquake. Compared to the Takatori

earthquake, the von Mises stress in the tank decreased by approximately 42%, 35%, and 41% under the Emeryville, Friuli, and Northridge seismic excitations, respectively, indicating a significant effect of input seismic intensity on storage tank performance.

- The ALE-based FSI modelling successfully captured transient stress variations induced and the free motion of the liquid at the top surface of the tank, critical in understanding seismic vulnerability.
- The Northridge earthquake resulted in the highest wave height of 24.1 cm when time reached at 17.20 seconds, while the Friuli and Emeryville events produced peaks of 17 cm and 18.7 cm, respectively.
- In the outer reinforced concrete containment tank, no significant damage was observed in the concrete compression as well as cracking in tension under seismic loads, confirming its structural resilience in the examined scenarios.

It should be noted that the water is used as an infilled liquid for simplification and comparisons purposes with code provision. The actual thermophysical properties of LNG tanks including lower density and viscosity compared to water would definitely affects the overall performance of the inner steel tanks. These findings have important implications for seismic design and safety assessment of LNG storage systems. The ALE approach is capable of capturing the complex interaction between inner tank wall and liquid domain. In particular, elevated sloshing heights that induces hydrodynamic convective pressure, which can increase the risk of roof impact, freeboard exceedance, and potential spillage or damage to internal components. Therefore, the evaluation of sloshing dynamics should be incorporated into performance-based seismic design approaches for LNG tanks, especially for sites with high seismicity.

Future Research Direction

The authors will conduct further studies with concentration on numerically simulating full-containment LNG tanks in actual cryogenic conditions in order to capture the impacts of thermal-structural interactions, which are essential for accurate seismic performance evaluation. Further understanding of foundation flexibility and ground motion amplification will also be possible with the incorporation of soil–structure interaction (SSI), which will result in more robust and dependable LNG tank design techniques. Additionally, the results from FEA will be compared with the different code provisions to identify the potential discrepancies in estimating the local buckling threshold, hydrodynamic pressure, and earthquake induced sloshing.

Acknowledgements

The authors gratefully acknowledge the Department of Civil Engineering at the University of North Dakota for providing access to the commercial finite element (FE) software ABAQUS, which was essential to perform this research.

References

1. 1. Y. Zhao, H.-N. Li, X. Fu, S. Zhang, and O. Mercan, “Seismic analysis of a large LNG tank considering the effect of liquid volume,” Shock Vib., vol. 2020, no. 1, pp. 1–13, 2020, Art. no. 8889055. https://doi.org/10.1155/2020/8889055
2. Q. Peng, H. Wu, R. F. Zhang, and Q. Fang, “Numerical simulations of base-isolated LNG storage tanks subjected to large commercial aircraft crash,” *Thin-Walled Struct.,* vol. 163, p. 107660, 2021. https://doi.org/10.1016/j.tws.2021.107660
3. S. Ullah and I. H. P. Mamaghani, “Numerical investigation on buckling response of cylindrical steel storage tanks under static loading,” *in Proc. 9th International Conference on Civil Structural and Transportation. Engineering* (ICCSTE 2024), Toronto, ON, Canada, June 13–15, 2024, Paper No. 251: https://doi.org/10.11159/iccste24.251
4. S. Ullah, N. Mwaura, and I. H. P. Mamaghani, “Nonlinear finite element analysis of flexible liquid-filled cylindrical steel storage tanks subjected to seismic excitations,” *Int. J. Civil Infrastruct.,* vol. 7, pp. 163-171, 2024: https://doi.org/10.11159/ijci.2024.017
5. S. Ullah and I. H. P. Mamaghani, “Numerical investigation on buckling response of cylindrical steel storage tanks under seismic excitation,” *European Association on Quality Control of Bridges and Structures – Digital Transformation in Sustainability,* EUROSTRUCT 2023: vol. 6, no. 5, pp. 343–347, Sept. 2023. DOI: https://doi.org/10.1002/cepa.1999
6. S. Ullah and I. H. P. Mamaghani, “Numerical investigation on buckling response of cylindrical steel storage tanks tanks under seismic excitation,” *European Association on Quality Control of Bridges and Structures – Digital Transformation in Sustainability,* EUROSTRUCT 2023: vol. 6, no. 5, pp. 343–347, Sept. 2023. DOI:

https://doi.org/10.1002/cepa.1999
7. Y. Zhao and Y. Lin, “Buckling of cylindrical open-topped steel tanks under wind load,” *Thin-Walled Struct*., vol. 79, pp. 83–94, 2014. https://doi.org/10.1016/j.tws.2014.02.010
8. G. Pórtela and L. A. Godoy, “Wind pressures and buckling of cylindrical steel tanks with a dome roof,” J. Constr. Steel Res., vol. 61, no. 6, pp. 808–824, 2005: https://doi.org/10.1016/j.jcsr.2004.11.001
9. S. Ullah and I. H. P. Mamaghani, “Numerical assessment and seismic performance evaluation of thin-walled cylindrical liquid-filled steel storage tanks supported on rigid soil,” in *Proceedings of the Annual Stability Conference, Structural Stability Research Council (SSRC)*, Louisville, Kentucky, Apr. 1–4, 2025.
10. Z. Chen, Z. Xu, L. Teng, J. Fu, T. Xu, and Z. Zhao, “Experimental and numerical investigation for seismic performance of a large-scale LNG storage tank structure model,” *Appl. Sci.,* vol. 12, no. 17, p. 8390, 2022. https://doi.org/10.3390/app12178390
11. S. Ullah and I. H. P. Mamaghani, “Numerical analysis of seismic response of steel cylindrical LNG storage tanks,” *in Proceedings of the 10th International Structural Engineering and Construction Conference (ISEC-10):* Innovative Theory and Practices in Structural Engineering and Construction, 2023, vol. 10, no. 1, 2023, https://doi.org/10.14455/ISEC.2023.10(1).OAG-01
12. D.-Y. Zhang and J.-Y. Wu, “Experimentally validated numerical analyses on the seismic responses of extra-large LNG storage structures,” Thin-Walled Struct., vol. 195, p. 111407, 2024. https://doi.org/10.1016/j.tws.2023.111407
13. S. Ullah and I. H. P. Mamaghani. Forthcoming. “Numerical analysis of seismic behavior in cylindrical steel storage tanks with liquid contents, involving fluid–structure interaction (FSI),” *ASCE J. Struct. Des. Constr. Pract.*, https://doi.org/10.1061/JSDCCC/SCENG-1770
14. W. Liu, C. Xiao, H. Zhou, and C. Wang, “Experimental investigation of liquid–tank interaction effects on full containment LNG storage tanks through shaking table tests,” Thin-Walled Struct., vol. 196, p. 111527, 2024. https://doi.org/10.1016/j.tws.2023.111527
15. S. Ullah and I. H. P. Mamaghani, “Numerical analysis of seismic vulnerability assessment of liquefied natural gas (LNG) cylindrical storage tanks involving fluid–structure interaction (FSI),” *in Proceedings of the CSCE 2025 Structures Specialty Conference*, Winnipeg, Manitoba, May 28–30, 2025.
16. S. Ullah, “Numerical investigation and seismic performance evaluation of liquefied natural gas (LNG) cylindrical steel storage tanks under earthquake loading”. *M.S. Thesis*, 6460, University of North Dakota, Grand Forks, ND, 2024. https://commons.und.edu/theses/6460
17. N. Sharari, B. Fatahi, A. Hokmabadi, and R. Xu, “Seismic resilience of extra-large LNG tank built on liquefiable soil deposit capturing soil–pile–structure interaction,” *Bull. Earthquake Eng.*, vol. 20, no. 7, pp. 3385–3441, 2022. https://doi.org/10.1007/s10518-022-01384-1
18. M. Souli, A. Ouahsine, and L. Lewin, “ALE formulation for fluid–structure interaction problems,” Computer Methods in Applied Mechanics and Engineering, vol. 190, no. 5–7, pp. 659–675, 2000. [Online]. Available: https://doi.org/10.1016/S0045-7825(99)00432-6
19. T. Nomura and T. J. R. Hughes, “An arbitrary Lagrangian–Eulerian finite element method for interaction of fluid and a rigid body,” Computer Methods in Applied Mechanics and Engineering, vol. 95, no. 1, pp. 115–138, 1992. [Online]. Available: https://doi.org/10.1016/0045-7825(92)90085-X
20. M. Souli and J. P. Zolésio, “Finite element method for free surface flow problems,” Computer Methods in Applied Mechanics and Engineering, vol. 129, no. 1–2, pp. 43–51, 1996. [Online]. Available: https://doi.org/10.1016/0045-7825(95)00883-7
21. S. Basting, A. Quaini, S. Čanić, and R. Glowinski, “Extended ALE method for fluid–structure interaction problems with large structural displacements,” Journal of Computational Physics, vol. 331, pp. 312–336, 2017. [Online]Available: https://doi.org/10.1016/j.jcp.2016.11.043
22. ASTM International, Standard Specification for Pressure Vessel Plates, Carbon Steel, for Moderate-and Lower-Temperature Service, West Conshohocken, PA, USA: ASTM International, 2010. https://doi.org/10.1520/A0516_A0516M-17